Acta Crystallographica Section B
Structural Science, Crystal Engineering and Materials
ISSN 2052-5206

Strong positive and negative deviations from Vegard's rule: X-ray powder investigations of the three quasi-binary phase systems $BiSX_{1-x}Y_x$ (*X*, *Y* = Cl, Br, I)

Peter Schultz and Egbert Keller

Acta Cryst. (2014). B**70**, 372–378

Acta Crystallographica Section B: Structural Science, Crystal Engineering and Materials publishes scientific articles related to the structural science of compounds and materials in the widest sense. Knowledge of the arrangements of atoms, including their temporal variations and dependencies on temperature and pressure, is often the key to understanding physical and chemical phenomena and is crucial for the design of new materials and supramolecular devices. *Acta Crystallographica B* is the forum for the publication of such contributions. Scientific developments based on experimental studies as well as those based on theoretical approaches, including crystal-structure prediction, structure–property relations and the use of databases of crystal structures, are published.

Acta Crystallographica Section B
Structural Science, Crystal Engineering and Materials
ISSN 2052-5206

Strong positive and negative deviations from Vegard's rule: X-ray powder investigations of the three quasi-binary phase systems $BiSX_{1-x}Y_x$ (X, Y = Cl, Br, I)

Peter Schultz and Egbert Keller*

Kristallographie, Institut für Geowissenschaften der Universität Freiburg, Hermann-Herder-Strasse 5, 79104 Freiburg, Germany

Correspondence e-mail: egbert.keller@krist.uni-freiburg.de

Received 13 May 2013
Accepted 13 January 2014

Three quasi-binary phase systems, $BiSX_{1-x}Y_x$ (X, Y = Cl, Br, I; $0 < x < 1$), have been investigated by X-ray powder diffraction. All three systems show unlimited solubility. For $BiSCl_{1-x}Br_x$ and $BiSCl_{1-x}I_x$, strong positive and negative deviations from Vegard's rule are observed with respect to the lattice parameters a and c. They are qualitatively explained by the asymmetry of the X coordination polyhedron and by anion–anion repulsions. For $x < 0.32$ [$x > 0.32$] the $BiSCl_{1-x}I_x$ system mimics the behaviour of the $BiSCl_{1-y}Br_y$ [$BiSBr_{1-y}I_y$] system ($0 < y < 1$).

1. Introduction

In a quasi-binary system, $A_mB_n \ldots P_{p(1-x)}Q_{px} \ldots X_rY_s$, of unlimited solubility, the lattice parameters t (= a, b, c) of the single mixed phases are functions of the concentration parameter x. If $t(x)$ is linear, the lattice parameter is said to obey Vegard's law (Vegard, 1921; Vegard & Dale, 1928). Usually, for real systems, deviations from linearity (positive or negative ones) are observed for the $t(x)$ curves, which can be quantified by different 'deviation parameters' (Keller & Krämer, 2005), *e.g.* $\Delta t_{0.5}$, the difference between the experimental $t(0.5)$ value and the corresponding 'Vegard value', $(t(0) + t(1))/2$. In the common case of $t(x)$ being a polynomial function of approximately second order, $\Delta t_{0.5}$ is also the *maximal* vertical deviation, $\Delta t_x(\max)$, between $t(x)$ and the Vegard straight line. By comparing the $\Delta t_{0.5}$ values of numerous quasi-binary systems of unlimited solubility described in the literature, deviations with $|\Delta t_{0.5}|$ values > 0.05 Å have been classified as 'strong' (Keller & Krämer, 2005). A strong positive deviation ($\Delta t_{0.5}$ = 0.17 Å) was observed, *e.g.*, for $c(x)$ of $BiOBr_{1-x}I_x$ in the course of a powder diffraction investigation of the three quasi-binary systems $BiOX_{1-x}Y_x$ (X, Y = Cl, Br, I). As the structures of the end members of these systems consist of XBi_2O_2X 'sandwich' layers held together merely by van der Waals forces, the corresponding one-sidedness of the X coordination polyhedron has been held responsible for this strong deviation (Keller & Krämer, 2005).

We now have investigated by powder diffraction the three quasi-binary systems $BiSX_{1-x}Y_x$ (X, Y = Cl, Br, I), which are chemically (but not structurally) related to $BiOX_{1-x}Y_x$ (X, Y = Cl, Br, I). Understanding the results obtained and described below will again require a closer look at the structures of the end-members $BiSX$ (X = Cl, Br, I; Voutsas & Rentzeperis, 1980, 1984; Haase-Wessel, 1973). These can be described as packings of one-dimensionally infinite thin XBi_2S_2X rods which are mutually connected by secondary Bi—S and Bi—X bonds and van der Waals forces (see §3.2). The structures were originally published in their *Pnma* (BiSCl) or *Pnam* (BiSBr, BiSI), but are described within the

Table 1
Lattice parameters (Å) in the BiS$X_{1-x}Y_x$ systems; numbers given in italics refer to samples prepared from well defined BiSX and BiSY crystals.

x	a	b	c	x	a	b	c
$BiSCl_{1-x}Br_x$				0.202 (4)	8.062 (2)	4.035 (1)	9.898 (1)
0.000 (0)	7.750 (1)	3.9943 (6)	9.976 (1)	0.248 (5)	8.108 (2)	4.043 (1)	9.901 (2)
0.100 (4)	7.819 (6)	4.0019 (6)	9.934 (3)	0.302 (5)	8.168 (3)	4.053 (1)	9.904 (2)
0.200 (4)	7.874 (1)	4.0097 (3)	9.908 (1)	0.350 (5)	8.210 (3)	4.063 (1)	9.920 (3)
0.300 (5)	7.929 (7)	4.016 (1)	9.886 (3)	0.402 (5)	8.252 (3)	4.074 (1)	9.934 (4)
0.402 (5)	7.965 (1)	4.0233 (3)	9.869 (1)	0.500 (6)	8.318 (4)	4.091 (1)	9.976 (4)
0.500 (6)	8.008 (4)	4.030 (1)	9.861 (2)	*0.5008*	*8.322*	*4.0912*	*9.972*
0.5034	*8.006*	*4.0305*	*9.859*	0.601 (6)	8.373 (2)	4.109 (1)	10.037 (3)
0.550 (6)	8.025 (1)	4.0331 (4)	9.857 (1)	0.700 (5)	8.417 (2)	4.127 (1)	10.094 (2)
0.600 (6)	8.041 (1)	4.0354 (5)	9.852 (1)	0.806 (5)	8.452 (2)	4.143 (1)	10.150 (2)
0.651 (5)	8.055 (1)	4.0396 (4)	9.852 (1)	0.900 (4)	8.486 (2)	4.160 (1)	10.202 (3)
0.700 (5)	8.074 (5)	4.043 (1)	9.850 (3)	1.000 (0)	8.513 (1)	4.176 (1)	10.262 (2)
0.749 (5)	8.082 (1)	4.0449 (3)	9.852 (2)				
0.801 (5)	8.096 (1)	4.0488 (1)	9.850 (1)	$BiSBr_{1-x}I_x$			
0.851 (5)	8.099 (3)	4.049 (1)	9.850 (2)	0.000 (0)	8.155	4.0643	9.860
0.900 (4)	8.119 (5)	4.058 (3)	9.853 (3)	0.116 (4)	8.216 (1)	4.077 (1)	9.896 (1)
0.950 (4)	8.141 (2)	4.060 (1)	9.852 (2)	0.203 (4)	8.262 (2)	4.088 (1)	9.930 (1)
1.000 (0)	8.155 (1)	4.0643 (2)	9.860 (2)	0.301 (5)	8.299 (1)	4.097 (1)	9.962 (1)
				0.402 (5)	8.347 (1)	4.1111 (3)	10.010 (1)
$BiSCl_{1-x}I_x$				0.501 (6)	8.372 (2)	4.119 (1)	10.042 (2)
0.000 (0)	7.750 (1)	3.9943 (6)	9.976 (1)	*0.5000*	*8.376*	*4.1192*	*10.046*
0.025 (2)	7.795 (1)	3.9989 (3)	9.957 (1)	0.600 (6)	8.405 (3)	4.130 (1)	10.090 (2)
0.049 (3)	7.839 (1)	4.0027 (4)	9.940 (1)	0.702 (5)	8.442 (2)	4.144 (1)	10.140 (2)
0.075 (3)	7.879 (2)	4.0082 (5)	9.925 (2)	0.800 (5)	8.470 (1)	4.1563 (4)	10.186 (1)
0.107 (3)	7.930 (1)	4.0150 (3)	9.914 (1)	0.900 (4)	8.492 (2)	4.1659 (7)	10.218 (2)
0.150 (4)	7.986 (3)	4.024 (1)	9.902 (2)	1.000 (0)	8.513 (1)	4.176 (1)	10.262 (2)

scope of this article uniformly in the *Pnma* setting, where the short lattice vector of magnitude ~ 4 Å is ***b*** and the aforesaid XBi$_2$S$_2$$X$ rods run parallel to [010]. Belonging to the same structure type ($PbCl_2$), the three structures form a crystal-chemically isotypic series, within which only X varies. The series shows a 'lattice parameter anomaly' inasmuch as the c parameter for the BiSBr phase is *smaller* than that of the BiSCl phase. This anomaly and the other geometrical changes within the series have been rationalized by Keller & Krämer (2006*b*).

2. Experimental

The preparation and investigation of BiS$X_{1-x}Y_x$ samples for numerous different x values required, in the first place, the synthesis of the three end-members, BiSX (X = Cl, Br, I). BiSCl (BiSBr) powders were synthesized from commercially available $BiCl_3$ ($BiBr_3$) and Bi_2S_3, the latter and BiSI were prepared from the elements. Furthermore, for the preparation of some extra BiS$X_{1-x}Y_x$ samples with x = 0.5, well defined BiSX crystals were grown.

2.1. Syntheses and crystal growth of BiSX (X = Cl, Br, I)

Bismuth sulfide (Bi_2S_3): 6.001 g (28.71 mmol) Bi (Chempur, 5 N) and 1.381 g (43.07 mmol) S (broken lump, Alfa, 5N) were sealed in an evacuated quartz ampoule of 30 mm diameter and 120 mm length. The ampoule was wrapped in a sheet of Fiberfrax and heated to 673 K for 5 d in a tube furnace. After cooling to room temperature and opening of the ampoule we obtained 7.343 g (14.28 mmol = 99.5%) of Bi_2S_3. A powder diffractogram of a mortared sample showed Bi_2S_3 to be the only (crystalline) product.

Bismuth sulfide chloride (BiSCl) (bismuth sulfide bromide, BiSBr): 3.15 g (10.00 mmol) $BiCl_3$ [3.34 g (7.44 mmol) $BiBr_3$] (both Alfa Aesar, 3N) were taken from the hitherto unopened supplier's flask and sealed immediately in an evacuated quartz ampoule of 10 mm diameter and 300 (180) mm length. The ampoule was placed into a vertically oriented one-zone tube furnace. The lower end with the material was heated to 463 (503) K, the temperature at the upper end (at the tube's end) happened to be 433 (473) K. After 2 (1) months most of the material had been transported to the upper end. To avoid contamination of this product with the non-volatile residue in the lower half the upper half of the ampoule was separated (by welding) to form a separate ampoule. The lower half contained 90 (330) mg of residual material. The ampoule containing the sublimated $BiCl_3$ ($BiBr_3$) was opened under Ar. To the 3.060 g (9.70 mmol) [3.01 g (6.71 mmol)] of the purified $BiCl_3$ ($BiBr_3$) 4.030 g (7.84 mmol) [3.000 g (5.83 mmol)] Bi_2S_3 (see above) were added. The ampoule was put into a larger ampoule of 20 mm diameter and 200 mm length, which was sealed under vacuum and heated in a tube furnace for 2 (3) d to 623 K and for 1 d to 673 K (and finally for 2 d to 723 K). Excess $BiCl_3$ ($BiBr_3$) was removed from the reaction product in temperature gradients of 623/598 K for 2 d and 473/453 K for another 2 d (753/703 K for 4 weeks). Yield: 6.450 g (23.33 mmol = 99.2%) BiSCl [5.504 g (17.15 mmol = 98%) BiSBr]. A carefully measured powder diffractogram of a mortared sample showed that besides BiSCl a small impurity (< 0.5%) of BiOCl was present [that BiSBr was the only (crystalline) product].

Bismuth sulfide iodide (BiSI): 0.846 g (4.05 mmol) Bi (Chempur, 5N), 0.129 g (4.02 mmol) S (broken lump, Alfa, 5N) and 0.523 g (2.06 mmol) I_2 (Merck Suprapur) were sealed in an evacuated quartz ampoule and heated to 673 K for 3 d. Then the ampoule was placed in a two-zone half shell furnace with vertical arrangement of the halves and exposed to a temperature gradient of 723/673 K for 7 d. After that time a network of prismatic BiSI crystals had grown in the colder part of the ampoule. Excess BiI_3 and some BiSI were removed by applying a temperature gradient of 573/523 K for 5 d; yield: 1.402 g (3.81 mmol = 94.8%). A carefully measured powder diffractogram of a mortared sample showed BiSI to be the only (crystalline) product.

Growth of BiSCl crystals: 2.8 g of BiSCl powder were sealed in an evacuated quartz ampoule. The ampoule was placed in a two-zone half shell furnace with vertical arrangement of the

halves and exposed to a temperature gradient of 758/713 K (note: decomposition temperature of BiSCl at normal conditions = 743 K). After 7 weeks large crystal needles of BiSCl had grown on the bulk (seated in the hotter part of the ampoule) and, to a much lesser extent, on the coolest part of the ampoule wall (together with $BiCl_3$). By breaking off from the bulk, 399 mg (14%) of well defined acicular crystals of BiSCl were obtained.

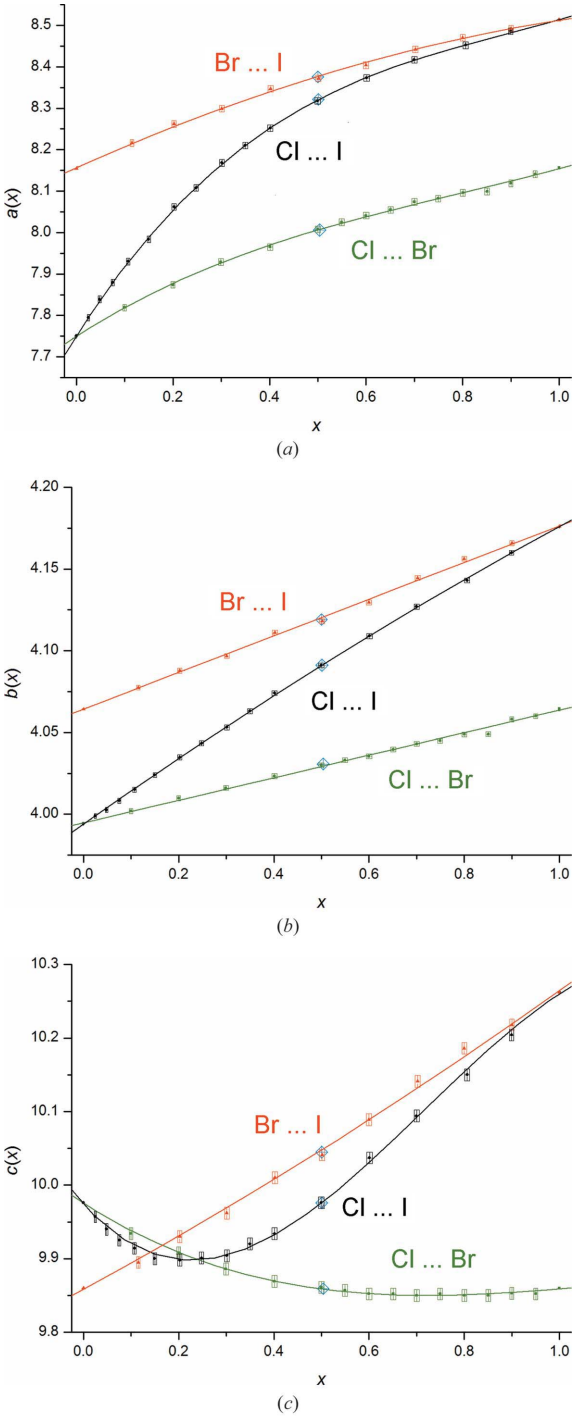

Figure 1
The functions $a(x)$, $b(x)$ and $c(x)$ in the systems $BiSCl_{1-x}Br_x$ ('Cl···Br'), $BiSCl_{1-x}I_x$ ('Cl···I') and $BiSBr_{1-x}I_x$ ('Br···I'). Blue rhombs represent samples prepared from well defined Bi*SX* and Bi*SY* crystals.

Growth of BiSBr (BiSI) crystals: 250 mg of BiSBr (BiSI) were sealed in an evacuated quartz ampoule of 12 mm internal diameter and 130 mm length, and exposed to a temperature gradient of 773/733 K (683/633 K) for 1 month. After that time BiSBr (BiSI) crystals had grown in the colder part of the ampoule. Yield: 33 mg (13%) BiSBr [108 mg (43%) BiSI] well defined acicular (thin prismatic) crystals.

2.2. Preparation and investigation of $BiSX_{1-x}Y_x$ samples

Various 100 ± 2 mg mixtures of Bi*SX*/Bi*SY* were made by weighing the appropriate amounts of Bi*SX* and Bi*SY* powders and mortaring the two weighed components. Each mixture was sealed in an evacuated quartz ampoule of about 5 mm diameter and 40 mm length. The ampoule was heated to 673 K for 2–3 d. The reaction product was mortared and, in most cases, a sample was measured on a Stoe Stadi-P powder diffractometer. The remaining product was sealed in another ampoule, heated to 673 K for another 2–3 d and measured again on the diffractometer. Indexing of the powder patterns and refinement of the lattice parameters were performed with the *WinXPOW* suite of programs (Stoe & Cie, 2004). If two diffraction patterns had been measured from a mixture, the two lattice parameter sets obtained were averaged. Final values are collected in Table 1 and visualized in Fig. 1 by means of the *Origin 7.0* software (OriginLab, 2002). Widths of the error boxes in Fig. 1 were derived as described by Keller & Krämer (2005), assuming that impurities in the educts did not exceed 2% (molar). From repeated diffractometer measurements of selected samples, the heights of the error boxes have been set to 0.008 Å for the $a(x)$ and $c(x)$ curves and 0.0015 Å for the $b(x)$ curves. Also by means of *Origin 7.0*, $t(x)$ curves of third order maximally were determined from the lattice parameter data with the pure compounds counted with fivefold weight (Table 2). $x(\Delta t_{max})$ values (Table 3) were found by determining the zeroes of the first derivatives of the functions $t(x) - t_V(x)$ with $t_V(x)$ representing the corresponding linear Vegard function.

As a check for the validity of our results obtained from mixing Bi*SX* powders (possibly suffering from amorphous impurities leading to tampered calculated x values), we prepared additional $BiSX_{0.5}Y_{0.5}$ samples from the well defined Bi*SX* and Bi*SY* crystals (assumed to be chemically 'pure'). Data points for the three samples fit well into the nine $t(x)$ curves (blue rhombs in Fig. 1; see also Table 1). Note that this does not necessarily prove that the educt powders used to prepare all the other mixtures actually were 'pure'. It only proves that the impurity amounts in all three educt materials (expressed in mol%) were (nearly) equal. Fulfillment of this condition implies, however, that 'true' $t(x)$ functions were obtained.

Note: preparation and measurement of most $BiSX_{1-x}Y_x$ mixtures have already been performed in 2010 (Schultz, 2010). The powder diffractogram of a $BiSCl_{0.65}I_{0.35}$ mixture prepared from BiSCl and BiSI samples stored since then (*i.e.* for ∼ 2 years) in unsealed containers showed – reproducibly – a superposition of the two diffractograms for $BiSCl_{\simeq 0.75}I_{\simeq 0.25}$

Table 2
Parameters A and B_i (Å) quantifying the fitting curves $A + B_1x + B_2x^2 + B_3x^3$ and correlation coefficients R for the nine $t(x)$ functions of the order n.

$t(x)$	$X\cdots Y$	n	A	B_1	B_2	B_3	R
$a(x)$	Cl···Br	3	7.750 (2)	0.75 (2)	−0.60 (5)	0.25 (3)	1.000 (4)
	Cl···I	3	7.7506 (9)	1.83 (1)	−1.70 (3)	0.63 (2)	1.000 (2)
	Br···I	2	8.156 (1)	0.527 (8)	−0.170 (8)	–	1.000(3)
$b(x)$	Cl···Br	1	3.9947 (4)	0.0690 (6)	–	–	0.999 (1)
	Cl···I	2	3.9939 (2)	0.206 (1)	−0.024 (1)	–	0.9999 (6)
	Br···I	1	4.0643 (5)	0.1121 (7)	–	–	1.000 (1)
$c(x)$	Cl···Br	3	9.9754 (8)	−0.41 (1)	0.43 (2)	−0.13 (2)	0.999 (2)
	Cl···I	3	9.974 (1)	−0.71 (2)	1.86 (5)	−0.86 (3)	0.999 (4)
	Br···I	2	9.858 (2)	0.35 (1)	0.05 (1)	–	0.999 (5)

and $BiSCl_{\simeq 0.5}I_{\simeq 0.5}$. This finding would be compatible with a miscibility gap in the range $0.25 < x < 0.5$. Samples of BiSCl and BiSI were therefore synthesized anew using methods similar to those described above. Powder diffractograms of both compounds obtained showed no (crystalline) impurities. Several mixtures covering the aforesaid composition range were prepared from the freshly synthesized materials. All diffractograms of these mixtures showed the pattern of only one single $BiSCl_{1-x}I_x$ phase. Furthermore, another $BiSCl_{0.65}I_{0.35}$ sample prepared after submission of this article from the original educts (aged for about 3 years in the meantime) was again single-phase after processing. We lack understanding of these findings but report them anyway for the sake of completeness. In the following discussion we will, however, treat the 'temporary' miscibility gap as non-existent.

3. Results and discussion

3.1. The nine $t(x)$ functions

Fig. 1 shows that the end-members of all three quasi-binary $BiSX_{1-x}Y_x$ systems form solid solutions over the whole composition range ($0 < x < 1$). This behaviour could be expected for $BiSCl_{1-x}Br_x$ and $BiSBr_{1-x}I_x$, but not for $BiSCl_{1-x}I_x$: unlimited solubility is usually only observed if the difference in the atomic radii of the varying element does not exceed 15% (*e.g.* Vainshtein *et al.*, 1982; Wells, 1984). In our cases, differences in the ionic radii ($r_{Cl} = 1.81$, $r_{Br} = 1.95$, $r_I = 2.20$ Å; Shannon, 1976) are about 8% for Cl/Br and 12% for Br/I, but 20% for Cl/I. Correspondingly, in the three $BiOX_{1-x}Y_x$ (X, Y = Cl, Br, I) systems unlimited solubility was observed only for the Cl/Br and Br/I systems, while in $BiOCl_{1-x}I_x$ solubility is restricted to the range $0.74 < x < 1$ (Keller & Krämer, 2005).

In the $BiOX_{1-x}Y_x$ systems, generally polynomial functions of (practically first or) second order had been appropriate to model the $t(x)$ curves set up by the data points. For the $BiSX_{1-x}Y_x$ systems, in some of the nine different cases functions of third order had to be employed instead (Table 2). While b obeys, in all three systems, (approximately) Vegard's rule, strong deviations can be observed for a and c in the $BiSCl_{1-x}Br_x$ and $BiSCl_{1-x}I_x$ systems. Table 3 shows all $\Delta t_{0.5}$ values and – in the case of functions of order 3 – the maximal deviations Δt_x(max). By far the largest $|\Delta t|$ values are found in the $BiSCl_{1-x}I_x$ system ($\Delta a_{0.41} = +0.20$ Å and $\Delta c_{0.31} = -0.16$ Å).

Table 3
Deviations from linearity at $x = 0.5$, $\Delta t_{0.5}$ and maximal deviations, Δt_x(max) (Å), of the $t(x)$ functions (see Table 2) of the order n in the range $0 < x < 1$.

For functions of first (second) order, Δt_x(max) = 0 [$\Delta t_{0.5}$]. $x(\Delta t_{max})$ is the x value associated with Δt_x(max).

	$X\cdots Y$	n	$\Delta t_{0.5}$	Δt_x(max)	$x(\Delta t_{max})$
	Cl···Br	3	0.053	0.058	0.376
$a(x)$	Cl···I	3	0.188	0.195	0.405
	Br···I	2	0.043	–	–
	Cl···Br	1	–	–	–
$b(x)$	Cl···I	2	0.006	–	–
	Br···I	1	–	–	–
	Cl···Br	3	−0.056	−0.058	0.423
$c(x)$	Cl···I	3	−0.142	−0.156	0.314
	Br···I	2	−0.015		

3.2. Structural aspects and relationships within the BiS*X* series

Similar to BiO*X*, the coordination polyhedron of the *X* atom in the BiS*X* structures (Figs. 2, 3 and 4) is one-sided inasmuch as *X* forms the tip of a flat (almost) tetragonal pyramid, the base of which is defined by four Bi atoms. In this respect, BiO*X* and BiS*X* are clearly different from *e.g.* K*X*, where the *X* coordination polyhedron is 'isotropic' (*i.e.* octahedral) and a corresponding mixed crystal system, $KBr_{1-x}I_x$, shows (almost) linear $a(x)$ functions (Teatum & Smith, 1957). In BiS*X*, at the side opposite to the base of the pyramid, only *X*—S and *X*—*X* (for *X* = I) van der Waals forces are present. Relationships *within* the pyramid are also 'one-sided' to some extent: two Bi atoms at one side are bound to *X* by stronger primary bonds and the other two by weaker secondary bonds (see bond valences listed in Table 4). Owing to this and the lower crystal structure symmetry (orthorhombic *versus* tetragonal) the $BiSX_{1-x}Y_x$ systems are more complicated than the $BiOX_{1-x}Y_x$ systems. Attempts to explain the behaviour of the lattice parameters in the $BiSX_{1-x}Y_x$ systems first requires an understanding of the geometrical changes within the series. These changes have been tentatively rationalized by Keller & Krämer (2006*b*). Their arguments are briefly repeated in a somewhat modified and therefore, hopefully, more comprehensive manner in the following.

The most interesting of the structural changes is a lattice parameter anomaly, namely the decrease of c by 0.12 Å in the transition BiSCl → BiSBr. It can be explained as follows: when Cl (*e.g.* Cl^i and Cl^{iii} in Fig. 2) is replaced (quantitatively) by Br, the primary (Bi^i-X^i) and secondary Bi—*X* bonds ($Bi^{vii}-X^i$ and Bi^i-X^{iii}) elongate (note: for symmetry codes see Fig. 2). This and the increased repulsion experienced by X^i from S^i (also due to the larger *X* radius) leads to a virtual shift of the (010) projection of X^i (and rod B bound to it)

approximately parallel to [$\bar{1}$05] and to a shift of the projection of X^{iii} (and rod A) approximately parallel to [601] (see partial structures with dotted bond sticks in Fig. 3). The two shifts also elongate the secondary Bi—S bonds Bi^{i}—S^{iii} and Bi^{vii}—S^{i}. Clockwise $\simeq$3° rotations of rod B (rod A) about a *b* axis positioned at approximately S^{iv} [X^{iii}] (see curved arrows in Fig. 3) re-establish the former secondary Bi—S bond lengths. By the combination of these rotations with the aforesaid shifts the apparent rotation axes are moved approximately from S^{iv} to Bi^{iv} (rod B) and from X^{iii} to Bi^{vi} (rod A) (see curved arrows in Fig. 2). Finally, the primary bond to Br^{iii} (within rod A) also elongates and shifts Br^{iii} 'downwards' (in Fig. 3). This and the described $\simeq$3° rotations would not be possible if there were not 0.8 Å gaps between vicinal Cl atoms (*e.g.* Cl^{i} and Cl^{ii}) in BiSCl. The gaps are closed to a large extent (but not fully) by the process. The rotations of the XBi_2S_2X rods at the unit-cell corners relative to the one at $\frac{1}{2}$, *y*,$\frac{1}{2}$ cause the unit-cell axes to also rotate clockwise (by 1.5°). From Fig. 2 it can clearly be seen how mainly the rotation of rod B and that at the diagonally opposite corner of the unit cell, visualized by the blue arrows, reduce the size of the *c* parameter.

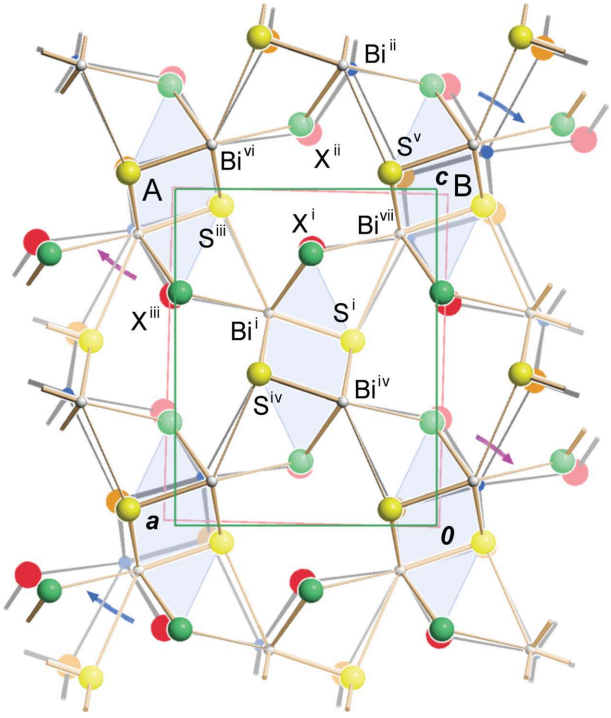

Figure 2
Superposition of the structures of BiSCl and BiSBr. Symmetry codes: (i) *x*, *y*, *z*; (ii) 1 − *x*, 1 − *y*, 2 − *z*; (iii) $\frac{1}{2}+x, y, \frac{3}{2}-z$; (iv) 1 − *x*, 1 − *y*, 1 − *z*; (v) $\frac{1}{2}-x, 1-y, \frac{1}{2}+z$; (vi) $\frac{3}{2}-x, \frac{1}{2}+y, \frac{1}{2}+z$; (vii) $-\frac{1}{2}+x, y, \frac{3}{2}-z$. Atoms/bonds at *y* = 0.75 (0.25) have been drawn darker (paler). Atom colours for BiSCl are: Bi: grey; S: yellow; Cl: green (all spheres shaded with three-dimensional effect). Colours for BiSBr are: Bi: blue; S: orange; Br: red (all spheres shaded plainly by using constant colour). The cross sections of the five central $ClBi_2S_2Cl$ rods have been emphasized by a light blue colour. All intra-rod bonds are primary and all inter-rod bonds are secondary bonds. The drawing is based on a similar one (Fig. 8 by Keller & Krämer, 2006*b*), but with ***a*** pointing in the opposite direction and with lattice parameters taken from powder refinement (Table 1). Curved arrows in the upper half symbolize the rotations of rod *A* (*B*) about a *b* axis near Bi^{vi} (Bi^{iv}). Arrows in the lower half denote two symmetry-equivalent rotations. Note that the vector $X^{i} \rightarrow X^{ii}$ makes an angle of $\sim$ 30° to the drawing plane.

Table 4
Bond valences for the bonds in BiS*X* as calculated by *softBV* (Adams, 2004).

Bond	BiSCl	BiSBr	BiSI
Primary Bi—S	0.70, 0.57	0.70, 0.56	0.73, 0.54
Secondary Bi—S	0.13	0.13	0.09
Primary Bi—*X*	0.32	0.34	0.37
Secondary Bi—*X*	0.14	0.14	0.14

The same mechanism is employed (in a modified manner) in the (imaginary) BiSBr → BiSI transition (Fig. 4), but here the *X*—*X* gaps become more than closed such that the rotation of the 'outer' rods stops at 1° and I—I repulsion as well as a substantial elongation of the secondary Bi—S bonds (reflected in the comparatively low formal bond valence of 0.09 in Table 4), this time 'incurable', are generated. It should be emphasized that generally in all three BiS*X* structures the anions are closely packed and S—S, S—*X* and I—I distances are equal to or below the radii sums. This is similar to (though more pronounced than) the BiO*X* structures but different from, *e.g.* the alkali halides *AX* (*A* = Na, K, Rb, Cs) where the anions (with the possible exception of I in NaI) are far from 'contacting' each other.

3.3. Possible explanations for *t*(*x*) curve shapes in $BiSCl_{1-x}Br_x$ and $BiSBr_{1-x}I_x$

As already stated above, we find strong deviations from Vegard's law in all three $BiSX_{1-x}Y_x$ systems. We first try to explain this qualitatively for the $BiSCl_{1-x}Br_x$ system: If one single Br atom in BiSBr (*e.g.* Br^{i} in Fig. 2) is replaced by a Cl

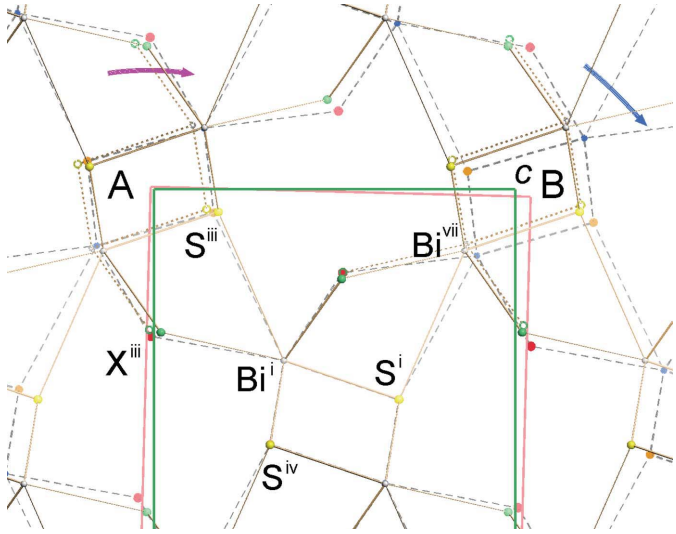

Figure 3
Detail from Fig. 2 redrawn with smaller sphere radii and bond stick thicknesses. Fully drawn bond sticks: BiSCl; dashed bond sticks: BiSBr; dotted bond sticks: shifted versions of rods *A* and *B* in BiSCl. Curved arrows symbolize the rotations of the shifted version of rod *A* (*B*) about a *b* axis near X^{iii} [S^{iv}].

atom, the primary Bi—X bonds (*e.g.* Bi^{i}—X^{i}) will shorten towards the Bi—X bond length known from BiSCl, but the necessary back-rotation of rod B to make the concurrent shortening of the secondary Bi—X bonds possible (*e.g.* Bi^{vii}—X^{i}), will be hindered by repulsion between S^{v} and Br^{ii}. The distance between these two anions (3.67 Å) is already below the sum of the two ionic radii (3.8 Å) and the rotation would shift S^{v} almost directly towards the midpoint between Br^{ii} and its duplicate in the next unit cell closer to the viewer. Thus, the two comparatively weak (see Table 4) secondary Bi—X bonds coinciding on the right side of the X^{i} coordination sphere in Fig. 2 shorten less than necessary (in contrast to the two primary bonds on the other side) and thus leave a above the straight line postulated by Vegard's law. On the other hand, there *will be* a certain shortening of this bond [otherwise $a(x)$ would be a roughly horizontal line for high x values], but it probably will be accomplished by a small *shift* of rod B approximately in the [100] direction instead of the expected back-rotation (thus avoiding too close a contact with Br^{ii}). This would explain the fact that c remains almost constant in the range $0.6 < x < 1$, thus leading to the large negative $\Delta t_{0.5}$ value for the $c(x)$ curve. Only when there is a chance that the second Br (Br^{ii}) has also been replaced by a Cl atom (*i.e.* at x values approaching 0.5), the rotation becomes possible and c can increase towards its value in BiSCl. Finally we will discuss the third $t(x)$ function: other than $a(x)$ and $c(x)$, the $b(x)$ function is almost linear. This can be understood from the fact that the coordination polyhedron of X is symmetrical in [010]: X lies on a (010) mirror (at least in the pure BiSX structures). Thus, bonding forces are of equal (or very similar) strength on both sides.

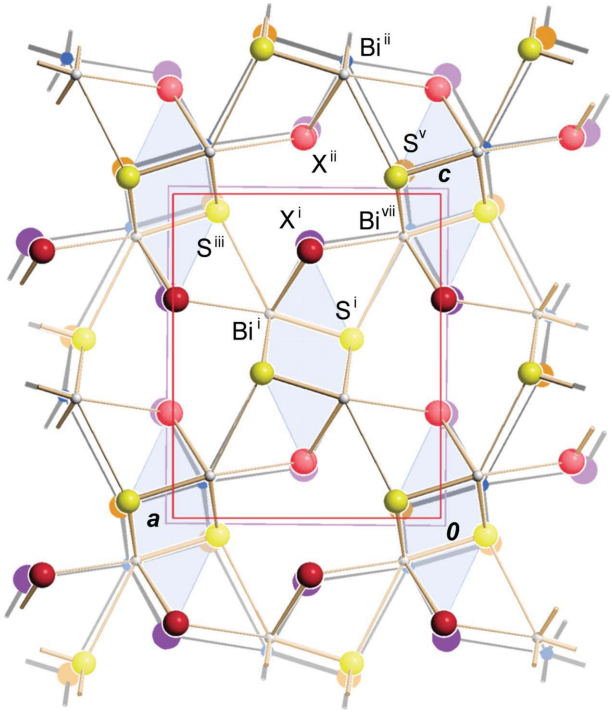

Figure 4
Superposition of the BiSBr and BiSI structures with lattice parameters taken from powder refinement results (Table 1). Atoms/bonds at $y = 0.75$ (0.25) have been drawn darker (paler). Atom colours for BiSBr are: Bi: grey; S: yellow; Br: red (spheres shaded with a three-dimensional effect). Atom colours for BiSI are: Bi: blue; S: orange; I: violet (spheres shaded with no three-dimensional effect).

In the $BiSBr_{1-x}I_x$ system, explanations for the strong positive deviation of $a(x)$ and the linearity of $b(x)$ are the same as before. However, c behaves differently here compared with $BiSCl_{1-x}Br_x$. First, c does not grow towards smaller x, but it shrinks as we do not have a lattice parameter anomaly in this system. Secondly, $c(x)$ is almost linear, although the X coordination polyhedron is highly unsymmetrical (*i.e.* one-sided) in the [001] direction. From the latter we would initially have predicted that, similar to $BiOBr_{1-x}I_x$ (Keller & Krämer, 2005), the shortening of the primary Bi^{i}—X^{i} bond (when I^{i} is replaced by Br) will not be followed by a move of I^{ii} towards Br^{i} large enough to fulfill Vegard's law, as this move is demanded by only weak van der Waals forces and thwarted by the supposed rigidity of the Bi—S framework (*cf.* Fig. 3 in Keller & Krämer, 2005). Things are different here though as the BiSI structure, unlike the BiOI (or the BiSBr) structure, is under tension in the [001] direction, built up by I—I repulsion (*e.g.* I^{i}—I^{ii} in Fig. 4), an effect which is indicated by the (too) small I—I distance (Keller & Krämer, 2006*b*) and by the elongation of the secondary Bi—S bonds (*e.g.* Bi^{i}—S^{iii} and Bi^{ii}—S^{v}). Thus, the strong force taking effect on Br^{i} on the lower side in Fig. 4 due to the shortening of the primary Bi^{i}—X^{i} bonds is accompanied by medium force trying to reduce the secondary Bi—S bonds to a normal length plus the (estimated) medium force of reducing the X—X distance due to decreased I—Br repulsion (compared with I—I repulsion). Both forces draw I^{ii} (and the atoms bonded to it) 'downwards' in Fig. 4, and, apparently, together are of similar power compared with the force on Br^{i}, which would explain why $c(x)$ is almost linear.

3.4. The $BiSCl_{1-x}I_x$ system

Undoubtedly the most remarkable of our experimental findings is the behaviour of the third system, $BiSCl_{1-x}I_x$. First the system forms solid solutions over the whole composition range, which is not as expected (see above). Secondly, the system exhibits very large deviations from linearity ($\Delta a_{0.42} = +0.20$, $\Delta c_{0.31} = -0.16$ Å). Thirdly, the system mimics to a high degree the behaviour of a combination of the two other systems: in the $0 < x < 0.32$ region the whole $BiSCl_{1-y}Br_y$ ($0 < y < 1$) system is emulated, and in the region $0.32 < x < 1$ we find an imitation of the whole $BiSBr_{1-y}I_y$ system (Fig. 5). The largest difference between $BiSCl_{1-x}I_x$ and the combination of the other two systems lies in the fact that the minimum of $c(x)$ in $BiSCl_{1-x}I_x$ (9.90 Å) exceeds c(BiSBr) = 9.86 Å by 0.04 Å, thus the $c(x)$ curve of $BiSCl_{1-x}I_x$ runs clearly above the combined $c(x')$ (with $x' = 0.32y$) and $c(x'')$ (with $x'' = 0.68y + 0.32$) curves of the other two systems, indicating that the maximal rotation of rods A and B (Fig. 2) is somewhat smaller than in the BiSCl → BiSBr case. This can easily be understood: if Cl^{i} (Fig. 2) is replaced by I instead of Br, the resulting larger shift of I^{i} in the [001] direction (due to the increased bond length to Bi^{i} and repulsion from S^{i}) plus larger

radius already closes the gap to Cl^{ii} (I^{i}—Cl^{ii} distance $\simeq$ 4.0 Å = sum of ionic radii, compared with Br^{i}—Cl^{ii} $\simeq$ 4.2 Å at a radii sum of 3.8 Å). Thus, subsequent rotation of the 'outer' rods, induced by the tenacity of the secondary Bi—S bonds and resulting in the *c* decrease, must stop at a smaller angle. Note that this rotation will leave the I—Cl distance below the radii sum, just as found for the I—I distance in the BiSI structure (4.1 *versus* 4.4 Å).

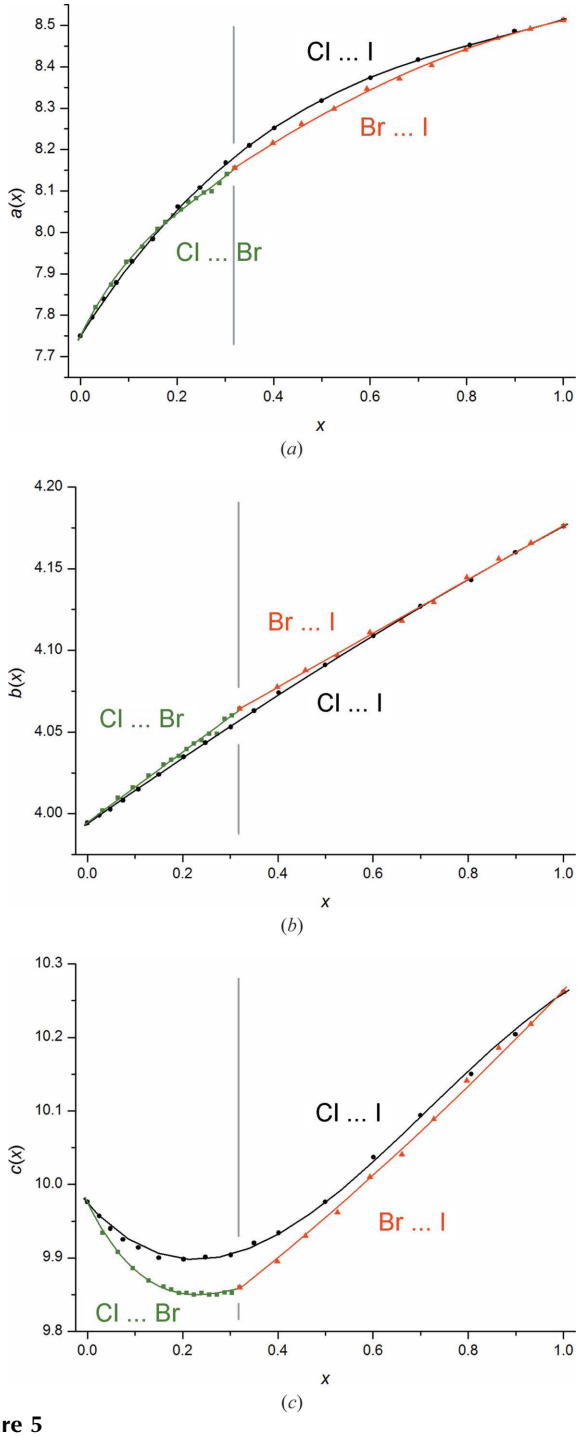

Figure 5
Comparison of the $t(x)$ functions of the $BiSCl_{1-x}I_x$ system with combinations of the corresponding $t(x')$ functions (with $x' = 0.32y$) of the $BiSCl_{1-y}Br_y$ and the $t(x'')$ functions (with $x'' = 0.68y + 0.32$) of the $BiSBr_{1-y}I_y$ systems ($0 < y < 1$). The grey vertical lines mark the transition point at $x = 0.32$.

In Fig. 5 the transition point (grey vertical lines) has been chosen as $x = 0.32$. It should be noted that for $a(x)$ [$b(x)$] alone, the optimal x value would have been 0.30 (0.35), thus 0.32 is a compromise. Apparently, when $\simeq$ 32% of the Cl atoms in BiSCl have been replaced by I, the system is mostly comparable to BiSBr. The value of $x \simeq 0.32$ matches roughly the ratio of 0.40 between the statistical size (radius) differences (Keller & Krämer, 2006*a*) $\rho_{Cl\,Br} = 0.150$ and $\rho_{Cl\,I} = 0.375$ Å: 0.15/0.375 = 0.40. Thus, this ratio is coarsely reflected in the shapes of the $t(x)$ curves of $BiSCl_{1-x}I_x$. Not surprisingly, the ratio between the corresponding BiS*X* lattice parameter *b* differences ($\Delta b_{ClBr} = 0.070$, $\Delta b_{ClI} = 0.182$ Å) is 0.38 and thus also in this range.

4. Conclusion

The general forms of the nine $t(x)$ curves for the three $BiSX_{1-x}Y_x$ systems, some of which showing strong positive or negative deviations from Vegard's law, can be qualitatively explained by comparing the forces acting on opposite sides of an *X* anion after it has replaced an *Y* anion. In some cases, anion–anion repulsions play an important role in the setup of such forces. The low *x* and high *x* parts of the $t(x)$ curves for the $BiSCl_{1-x}I_x$ system reflect with high agreement the corresponding curves of the other two systems.

We thank Ms Luitgard Rees-Isele and Mr Hans-Peter Winkler for technical assistance (especially in preparing the edducts BiS*X*, some of the investigated $BiSX_{1-x}Y_x$ mixtures and in growing the BiS*X* crystals) and two anonymous referees for helpful comments.

References

Adams, S. (2004). *softBV*. University of Göttingen, Germany, http://kristall.uni-mki.gwdg.de/softbv.
Haase-Wessel, W. (1973). *Naturwissenschaften*, **60**, 474.
Keller, E. & Krämer, V. (2005). *Z. Naturforsch. Teil B*, **60**, 1255–1263.
Keller, E. & Krämer, V. (2006*a*). *Acta Cryst.* B**62**, 411–416.
Keller, E. & Krämer, V. (2006*b*). *Acta Cryst.* B**62**, 417–423.
OriginLab (2002). *Origin*, Version 7.0303. OriginLab Corporation, Northampton, MA, USA.
Schultz, P. (2010). BSc thesis, Albert-Ludwigs-Universität Freiburg, Germany.
Shannon, R. D. (1976). *Acta Cryst.* A**32**, 751–767.
Stoe & Cie. (2004). *WinXPOW*, Version. 2.11. Stoe & Cie, GmbH, Darmstadt, Germany.
Teatum, E. T. & Smith, N. O. (1957). *J. Phys. Chem.* **61**, 697–698.
Vainshtein, B. K., Fridkin, V. M. & Indenbom, V. L. (1982). *Modern Crystallography*, Vol. II, p. 116. Berlin: Springer.
Vegard, L. (1921). *Z. Phys.* **5**, 17–26.
Vegard, L. & Dale, H. (1928). *Z. Kristallogr.* **67**, 148–162.
Voutsas, G. P. & Rentzeperis, P. J. (1980). *Z. Kristallogr.* **152**, 109–118.
Voutsas, G. P. & Rentzeperis, P. J. (1984). *Z. Kristallogr.* **166**, 153–158.
Wells, A. F. (1984). *Structural Inorganic Chemistry*, 5th ed., p. 1294. Oxford: Clarendon Press.